

# Prediction of Effectiveness Factor Using One-Dimensional Approximations for Complex Pellet Shapes and Abnormal Kinetics Expressions

Néstor J. Mariani,<sup>†,‡</sup> María J. Taulamet,<sup>†,‡</sup> Sergio D. Keegan,<sup>†</sup> Osvaldo M. Martínez,<sup>†,‡</sup> and Guillermo F. Barreto<sup>\*,†,‡</sup>

<sup>†</sup>PROIRQ, Departamento de Ingeniería Química, Facultad de Ingeniería, UNLP, La Plata, Argentina

<sup>‡</sup>Centro de Investigación y Desarrollo en Ciencias Aplicadas “Dr. J. J. Ronco” (CINDECA) CCT-La Plata-CONICET- UNLP, calle 47 No. 257, CP B1900AJK, La Plata, Argentina

**ABSTRACT:** This contribution undertakes the evaluation of one-dimensional (1D) models to approximate the behavior of actual three-dimensional (3D) catalyst pellets, in the case of abnormal kinetics and close to the limit of steady state multiplicity. Two 1D models are tested: a one parameter model, called generalized cylinder (1D-GC) and a three parameter model termed the variable diffusivity (1D-VD) model. A representative set of shapes presented by commercial catalytic pellets was selected to study the performance of the models to predict effective reaction rates. Kinetics expressions covering typical cases of thermal and self-inhibition effects have been considered. Predictions of effectiveness factor using 1D-GC and 1D-VD models are compared with numerical results obtained from the Comsol Multiphysics environment for the 3D pellets. The simpler 1D-GC model can lead to maximum errors exceeding 40%, while the 1D-VD model reduces them to a level of 10%.

## 1. INTRODUCTION

The intraparticle diffusion-reaction problem has been the focus of numerous studies as it is an important issue in modeling catalytic fixed beds. Mass conservation balances inside real pellets should normally be stated for two (2D) or three (3D) spatial coordinates, and a numerical solution must be performed. This computational task is affordable when a single set of conditions is undertaken, but even for the simplest practical case (e.g., simulation of a catalytic reactor with a single reaction), the calculations have to be repeated thousands of times. Besides, for modeling applications such as reactor optimization, the number of evaluations will increase by orders of magnitude. In addition, dealing with a set of reactions introduces a further computational burden. Thus, approaches that avoid the use of 2D or 3D computations are extremely valuable or even mandatory in most cases.

A first attempt to reduce the dimensionality of the problem was introduced by Aris<sup>1</sup> in 1965 showing that at large values of the Thiele modulus, the effectiveness factor for a single reaction does not depend on the pellet shape, but just on the ratio of pellet volume to external surface area,  $l$ . Then, to approximately evaluate the effectiveness factor at low and intermediate values of Thiele modulus, any simple 1D geometry satisfying the actual value of  $l$  could be adopted, as a slab of semiwidth  $l$  or a long circular cylinder of radius  $2l$ . Errors of around 20% should be expected using this approach for relatively simple kinetics expressions.

Datta and Leung<sup>2</sup> proposed a more convenient 1D model, here referred to as the generalized cylinder (1D-GC) model. It is supposed that diffusion takes place along a distance  $L$  (effective diffusion length) of a hypothetical body of cross section varying as  $z^\sigma$ , where  $z$  is the nondimensional coordinate. The suitable value of  $L$  is found by matching the value  $l$  of the

actual pellet and one additional property characterizing its shape provides the value for parameter  $\sigma$  (shape factor).

Macias et al.<sup>3</sup> employed the 1D-GC model to estimate effectiveness factor in hydrodesulfurization of diesel-fuels carried out over trilobe catalyst pellets. Recently, Lopes et al.<sup>4</sup> analyzed the diffusion-reaction problem in catalytic thin coatings supported on microchannels and a variety of kinetic expressions using successfully the 1D-GC approach.

Mariani et al.<sup>5–8</sup> focused the application of one-dimensional models for predicting the effectiveness factor in catalytic pellets of arbitrary shape in the packed bed reactors. In particular, for the 1D-GC model they proposed two different criteria to estimate the shape factor  $\sigma$  by requiring that the 1D-GC model match the behavior of the actual pellet either at low<sup>5</sup> or high<sup>6</sup> reaction rates. It is worth noting that when using the high reaction rate criteria  $\sigma$  can be straightforwardly obtained just from elementary geometric features of the pellet. The expected errors of the 1D-GC model employing the high reaction rate criteria is less than 3% for a variety of commercial shaped pellets with normal kinetic behavior, i.e. when the effectiveness factor decreases monotonically as the Thiele modulus increases.<sup>7,8</sup>

Nonetheless, it has been detected that even for isothermal linear kinetics the 1D-GC model becomes unable to accurately capture the behavior of shaped pellets when some ratios between their geometrical dimensions are modified up to a threshold value.<sup>9</sup> Therefore, to restore precision within 2% it

**Special Issue:** NASCRE 3

**Received:** February 22, 2013

**Revised:** April 25, 2013

**Accepted:** April 30, 2013

**Published:** April 30, 2013

was necessary to propose a new 1D model, called the variable diffusivity (1D-VD) model, which introduces three parameters evaluated by satisfying simultaneously the behavior of the actual pellet at high and low reaction rates.

The purpose of this contribution is to thoroughly test the effect of kinetic expressions on the prediction of effectiveness factor by one-dimensional models, extending the analysis up to near the limit of steady state multiplicity for a representative set of commercial pellets.

## 2. FORMULATION FOR THE EFFECTIVENESS FACTOR IN 3D PELLETS AND SERIES EXPANSIONS AT LOW AND HIGH THIELE MODULUS

A single catalytic reaction and the following restrictions will be considered to undertake the diffusion-reaction problem inside a pellet of arbitrary geometry:

- Uniform composition and temperature exist at the external surface of the pellet.
- The porous medium is isotropic as regards mass and heat transport properties.
- Mass fluxes and heat flux are described by Fick's and Fourier's laws with uniform effective diffusivities and thermal conductivity.
- Uniform catalytic activity exists.

Restrictions c and d can be removed at the expense of minor modifications in the description of the 3D problem and its approximation by 1D models. However, as case studies undertaken in this contribution satisfy those restrictions, they will be maintained for the sake of simplicity. Keegan et al.<sup>10,11</sup> presented an extended formulation for a general 3D problem removing restrictions c and d.

The flux of any species  $j$ , including a key species A (the limiting reactant is a suitable choice for A), can be written as  $\mathbf{N}_j = -D_j \nabla C_j$  and the heat flux as  $\mathbf{q} = -\lambda \nabla T$ , where  $D_j$  and  $\lambda$  are effective diffusivities and thermal conductivity, respectively.

Under assumptions a–c, molar concentrations and temperature can be related to the molar concentration of A, according to<sup>12</sup>

$$C_j = C_{j,s} + (\nu_j/\nu_A)(D_A/D_j)(C_A - C_{A,s}) \quad (1a)$$

$$T = T_s + \Delta H_A(D_A/\lambda)(C_A - C_{A,s}) \quad (1b)$$

where the suffix "s" stands for values at the external surface,  $\nu_j$  are stoichiometric coefficients, and  $(-\Delta H_A)$  is the heat of reaction per mole of A.

If the consumption rate of A ( $\pi_A$ ) is a known expression in terms of composition and temperature, eqs 1 and the condition  $\pi_A = 0$  will allow evaluating the molar concentration of A if chemical equilibrium is reached within the pellet,  $C_{A,e}$ , for given values  $C_{j,s}$  and  $T_s$ .

Defining the dimensionless concentration  $Y = (C_A - C_{A,e})/(C_{A,s} - C_{A,e})$ , the dimensionless reaction rate  $r(Y) = \pi_A/\pi_{A,s}$  will depend only on  $Y$ , for given values  $C_{j,s}$  and  $T_s$ . Note that  $0 \leq Y \leq 1$ ,  $r(0) = 0$  and  $r(1) = 1$ .

The steady state conservation equation for species A inside the catalytic pellet can be written

$$\nabla^{*2}(Y) = \Phi^2 r(Y), \text{ in } V_p \quad (2a)$$

$$Y = 1, \text{ on } S_p \quad (2b)$$

where  $V_p$  stands for either the spatial catalyst domain or its volume,  $S_p$  stands either for the external pellet surface or its

area, the dimensionless Laplacian operator  $\nabla^{*2}$  has been rendered dimensionless with the characteristic length  $l = V_p/S_p$ , and the Thiele modulus  $\Phi$  is defined as

$$\Phi^2 = l^2 \frac{\pi_{A,s}}{D_A(C_{A,s} - C_{A,e})} \quad (3)$$

The effectiveness factor is evaluated from

$$\eta = \frac{1}{V_p} \int_{V_p} r \, dV_p \quad (4)$$

**Series Expansion at Low Thiele Modulus.** The solution of eqs 2 at low Thiele modulus has been addressed in the literature.<sup>13</sup> A regular perturbation analysis can be carried out to expand  $\eta$  (eq 4) in powers of  $\Phi^2$ , leading to the following three-term truncated series expression:

$$\eta = 1 - r'(1)\gamma\Phi^2 + \left[ r'(1)^2 + \frac{1}{2}r''(1) \right] \beta\Phi^4 \quad (5)$$

where  $r'(1) = (dr/dY)_{Y=1}$ ,  $r''(1) = (d^2r/dY^2)_{Y=1}$ , and  $\gamma$  and  $\beta$  are expressed as

$$\gamma = \frac{\int_{V_p} G \, dV_p}{V_p} \quad (6a)$$

$$\beta = \frac{\int_{V_p} G^2 \, dV_p}{V_p} \quad (6b)$$

$G$  is the solution of

$$\nabla^{*2}G = -1, \text{ in } V_p \quad (7a)$$

$$G = 0, \text{ on } S_p \quad (7b)$$

It is worth noting that  $G$  (auxiliary field) does not depend on kinetics, hence the parameters  $\gamma$  and  $\beta$  depend only on the geometry of the pellet. The solution of problem 7 for  $G$  should be carried out only once for a given pellet shape.

**Series Expansion at High Thiele Modulus.** Assuming that  $S_p$  can be composed of smooth regions, i.e. surface pieces with continuous curvature radii, separated by edges, Keegan et al.<sup>10,11</sup> developed a formulation for problem described by eq 2 that allows expressing  $\eta$  for high Thiele modulus as a two-term truncated series in power of  $(1/\Phi)$ .

$$\eta = \frac{I_1}{\Phi} - \frac{I_2}{\Phi^2} \Gamma \quad (8)$$

where

$$I(Y) = 2 \int_0^Y r(Y_o) \, dY_o \quad (9a)$$

$$I_1 = [I(1)]^{1/2} \quad (9b)$$

$$I_2 = \frac{1}{I_1} \int_0^1 [I(Y)]^{1/2} \, dY \quad (9c)$$

The parameter  $\Gamma$ , which arises from the analysis presented by Keegan et al.,<sup>10,11</sup> accounts for the effect of the smooth regions and edges of the pellet and can be expressed as

$$\Gamma = \frac{l}{S_p} \left[ \int_{S_p} \mathcal{Y}_s \, dS + \int_W \omega(\theta) \, dW \right] \quad (10)$$

In eq 10  $\mathcal{Y}_s = 1/R_a + 1/R_b$ , where  $R_a$  and  $R_b$  are the local principal radii of curvature on the pellet surface with the following sign convention: positive if the center of curvature is oriented toward the inside of the catalyst and negative otherwise.

$W$  in eq 10 accounts for the total length of the edges and coefficient  $\omega$  depends very weakly on the type of reaction rate expression but strongly on the *intersecting angle*  $\theta$  that a pair of smooth regions defines when they meet at the edge. The following approximation was proposed by Keegan et al.<sup>11</sup> to estimate  $\omega$ :

$$\omega(\theta) = \begin{cases} \frac{b_0}{\theta} \left[ 1 - \left( \frac{\theta}{\pi} \right)^{\pi^2/b_0} \right], & \text{if } 0 \leq \theta \leq \pi \\ \frac{\pi^2 A}{(\pi - A)\theta + \pi(2A - \pi)} \left[ 1 - \frac{\theta}{\pi} \right], & \text{if } \pi < \theta \leq 2\pi \end{cases} \quad (11)$$

where  $b_0 = 5.2I_1^{0.3}/I_2^{0.1}$  and  $A = -\omega(2\pi) = 1.9/(I_1 I_2)^{0.07}$ .

Concerning eq 10, it is worth mentioning that almost all pellet shapes show smooth regions with constant curvatures, hence the integral on  $S_p$  is very easily evaluated by adding the contribution of each region. Besides, the edges normally present constant intersecting angles  $\theta$  and the second integral in eq 10 can also be straightforwardly evaluated. The effect of kinetics on  $\Gamma$  is introduced in eq 11 by parameters  $I_1$  and  $I_2$  (eqs 9). Detailed examples on the procedure to estimate  $\Gamma$  from eq 10 for different 3D bodies can be found in the works of Mariani et al.<sup>8</sup> and Keegan et al.<sup>11</sup> In general, the geometric information needed for such calculations is basically the same as needed to evaluate the volume and external surface area of the 3D pellet.

### 3. DESCRIPTION OF 1D MODELS

The main features of both, 1D-GC and 1D-VD, models will be outlined in the following paragraphs.

**Generalized Cylinder Model (1D-GC).** The 1D-GC model can be envisaged as a solid body that allows material and heat transport in only one spatial coordinate  $z'$  and presents a variable cross-section  $S(z)$ :

$$S(z) = S_p \left( \frac{z'}{L} \right)^\sigma = S_p z^\sigma$$

where  $S_p$  is the external surface area of the actual pellet. Symmetry applies at  $z = 0$  and the external surface is at  $z = 1$ , where the model's cross-section coincides with the external surface area of the actual pellet,  $S(1) = S_p$ .

For a reactant A with dimensionless concentration  $Y$  and reaction rate  $r(Y)$ , as defined in section 2, the mass conservation balance according to the 1D-GC model can be written as

$$z^{-\sigma} \frac{d}{dz} \left( z^\sigma \frac{dY}{dz} \right) = \left( \frac{L}{l} \right)^2 \Phi^2 r(Y) \quad (12a)$$

$$Y = 1 \quad \text{at} \quad z = 1 \quad (12b)$$

$$dY/dz = 0 \quad \text{at} \quad z = 0 \quad (12c)$$

where the Thiele modulus  $\Phi$  is the same as in the actual pellet (eq 3).

The 1D-GC model encompasses the classical 1D problems in a slab ( $\sigma = 0$ ), an infinitely long circular cylinder ( $\sigma = 1$ ), and a sphere ( $\sigma = 2$ ).

The effectiveness factor for the hypothetical pellet is

$$\eta^{1D-GC} = (1 + \sigma) \int_0^1 r(Y) z^\sigma dz \quad (13)$$

To define  $L$ , the volume of the 1D-GC body should equal the actual pellet volume  $V_p$ . As the external surface area was chosen as that of the actual pellet ( $S_p$ ), this requirement corresponds to maintaining the same characteristic length  $l$  as the actual pellet:

$$V^{1D-GC} = \int_0^L S_p \left( \frac{z'}{L} \right)^\sigma dz' = \frac{S_p L}{\sigma + 1} \quad (14)$$

From  $V^{1D-GC} = V_p$ , it follows that

$$L = (1 + \sigma)l \quad (15)$$

Equation 15 allows  $\eta^{1D-GC}$  to match the limiting values of  $\eta$  at very high values of  $\Phi$ , i.e.,  $\eta^{1D-GC} \rightarrow I_1/\Phi$  (see eq 8) as  $\Phi \rightarrow \infty$ . On the other hand, the use in the 1D-GC model of the same  $\Phi$  value as in the actual pellet just warrants that  $\eta^{1D-GC} \rightarrow 1$  as  $\Phi \rightarrow 0$ . Therefore, the value of the shape factor  $\sigma$  can be evaluated by matching the second term of either the low- $\Phi$  (eq 5) or the high- $\Phi$  (eq 8) expansion series of both, actual pellet and 1D-GC model.

If the low- $\Phi$  series is used as a criterion for fixing  $\sigma$ , it can be shown that in eq 5  $\gamma^{1D-GC} = (1 + \sigma)/(3 + \sigma)$ . Using  $\gamma^{1D-GC} = \gamma$  (the value of the actual pellet), we obtain

$$\sigma = \frac{3\gamma - 1}{1 - \gamma} \quad (16)$$

Similarly,  $\Gamma^{1D-GC} = \sigma/(1 + \sigma)$  in eq 8 and the high- $\Phi$  criterion leads to

$$\sigma = \frac{\Gamma}{1 - \Gamma} \quad (17)$$

where  $\Gamma$  is the second term coefficient in eq 8 for the actual pellet.

Hereafter, the 1D-GC model will be denoted 1D-GC $\gamma$  or 1D-GC $\Gamma$ , according to the use of eq 16 or eq 17, respectively, to fix  $\sigma$ .

**Variable Diffusivity Model (1D-VD).** The 1D-VD model is based on a hypothetical pellet allowing mass transport along only one spatial Cartesian coordinate  $x'$  spanning from the external surface ( $x' = 0$ ) to the symmetry position  $x' = L$ , i.e. as for a slab of half-thickness  $L$ . The dimensionless coordinate is defined as  $x = x'/L$ . The diffusivity of the key species A is assumed to vary with  $x$  according to

$$D_A \Theta(x), \Theta(0) = 1 \quad (18)$$

where  $\Theta(x)$  is some positive function containing free parameters to match the behavior of a given 3D pellet described in section 2. Restriction  $\Theta(0) = 1$  provides a convenient normalization, without loss of generality. When kinetics depends intrinsically on the concentrations of other species  $j$ , the diffusivity for them should also be affected by  $\Theta(x)$ , i.e.,  $D_j \Theta(x)$  is to be employed.

We assume for the actual pellet a dimensionless reaction rate  $r(Y)$  for species A, a Thiele modulus  $\Phi$ , and characteristic length  $l$ . Using the same set of variables for the 1D-VD model, it is obtained for the conservation equation of species A

$$\frac{d}{dx} \left[ \Theta(x) \frac{dY}{dx} \right] = \Phi^2 r(Y) \quad (19a)$$

$$Y = 1 \quad \text{at} \quad x = 0 \quad (19b)$$

$$dY/dx = 0 \quad \text{at} \quad x = 1 \quad (19c)$$

where the condition  $L = l$  has already been employed in eq 19a.

The effectiveness factor can be obtained using the following expression:

$$\eta^{1D-VD} = \int_0^1 r(Y) dx \quad (20)$$

Without any further specification for  $\Theta(x)$ , the model satisfies the first terms ( $\eta^{1D-VD} \rightarrow 1$  as  $\Phi \rightarrow 0$ ;  $\eta^{1D-VD} \rightarrow \mathcal{I}_1/\Phi$  as  $\Phi \rightarrow \infty$ ) in the series expansions (eqs 5 and 8) of the actual pellet at low and high Thiele modulus. We state now that the 1D-VD model should satisfy the two additional terms of the truncated low- $\Phi$  series (eq 5) and the second term of the truncated high- $\Phi$  series (eq 8). This is to say, parameters  $\gamma$ ,  $\beta$ , and  $\Gamma$  of the 1D-VD model should coincide with those of the actual pellet. To this end, we choose  $\Theta(x)$  as a three-parameter function, according to the following expression

$$\Theta(x) = \exp(C_1 x + C_2 x^\alpha) \quad (21)$$

where  $C_1$ ,  $C_2$ , and  $\alpha$  are the fitting parameters.

Choosing a variable diffusivity model and the specific exponential form in eq 21 obeys to the possibility of fitting simultaneously the three shape parameters  $\gamma$ ,  $\beta$ , and  $\Gamma$  of an actual pellet without any restriction for their relative values (details can be found in Mocciano's doctoral dissertation<sup>14</sup>).

Equating terms of the same order in the series expansions of the actual pellet and 1D-VD model, the following expressions are derived:

$$\Gamma = - \left[ \frac{1}{2} \frac{d\Theta(x)}{dx} \right]_{x=0} = -\frac{1}{2} C_1 \quad (22a)$$

$$\gamma = \int_0^1 \frac{(1-x)^2}{\Theta(x)} dx \quad (22b)$$

$$\beta = \int_0^1 F^2(x) dx, \quad F(x) = \int_0^x \frac{1-x_0}{\Theta(x_0)} dx_0 \quad (22c)$$

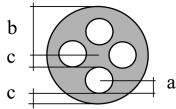
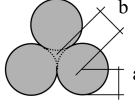
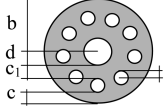
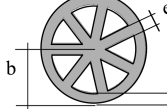
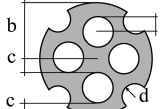
where  $\Gamma$ ,  $\gamma$ , and  $\beta$  are the values of the actual 3D pellets calculated from eqs 6a, 6b, and 10.

$C_1$  is immediately obtained from 22a,  $C_1 = -2\Gamma$ , while eqs 22b and 22c are to be simultaneously solved for  $C_2$  and  $\alpha$ . We found it convenient to nest iterations by guessing the value of  $\alpha$  (always  $\alpha > 1$ ), solving 22b for  $C_2$  and repeating the  $\alpha$ -guess until satisfaction of eq 22c.

#### 4. RESULTS

A representative set of shapes corresponding to commercially available catalysts (trilobe, 4-holes, wagon wheel, 10-holes, modified 4-holes) were selected. The selection of the shapes showing multiple internal holes was also driven by the fact that they lead to the largest errors when using 1D approximations for isothermal first order reactions.<sup>7,9</sup> The selected shapes are intended for a variety of chemical processes, like oxidations, hydrogenations, isomerizations, hydrotreatments, steam reforming, etc. Table 1 summarizes shapes and dimensions of the catalyst pellets used in this work, which have been taken from manufacturers' catalogues (e.g., Haldor Topsoe, Johnson

**Table 1. Cross-sections and Geometrical Parameters of the Analyzed Pellets ( $y = a/b$ ;  $h = H/(H + b)^a$ )**

Pellet	Cross section	Dimensions
4-holes		$y=0.273$ $c=0.833 a$ $h=0.645$
Trilobe		$y=0.866$ $h=0.684$
10-holes		$y=1/8$ $c=1.6 a$ $c_1=2.4 a$ $d=2 a$ $h=0.615$
Wagon wheel		$e=0.2 b$ $h=0.477$
Modified 4-holes		$y=1/4$ $c=a$ ; $d=0.831 a$ $h=0.723$

<sup>a</sup> $H$  stands for the pellet height.

Matthey, etc.). However, ratios between dimensions can show differences from those given in Table 1. As an specific example of such differences, the effect of pellet height  $H$  has been analyzed by considering two values: those leading to the finite ratios in Table 1 and  $H \rightarrow \infty$  [i.e.,  $h = 1$  in terms of the dimensionless variable  $h = H/(H + b)$  in Table 1]. The reason for choosing the second case can be explained by noting that for the opposite situation,  $H \rightarrow 0$ , any particle behaves as a slab, irrespective of the cross-section shape. Consequently, any of the 1D models ( $\sigma = 0$  for the 1D-GC model and  $\Theta(z) \equiv 1$  for the 1D-VD model) will produce the exact value of  $\eta$ , as the mass fluxes are 1D. The maximum effect of the cross-section shape is therefore exerted when  $H \rightarrow \infty$ , and this extreme involves, for some specific cross-shapes, the highest levels of errors found from using 1D models. Nonetheless, it should be mentioned that the maximum error is not always found for  $H \rightarrow \infty$ . For example for the circular cylinder, mass fluxes are also 1D along the radial coordinate when  $H \rightarrow \infty$  and the largest deviations occur at intermediate values of  $H$ .

Abnormal kinetics (i.e. those which go through a maximum reaction rate as reaction proceeds) are undertaken in this study, as they show high parametric sensitivity and represent the most challenging cases for approximations like the 1D models treated here. It is well-known that abnormal behavior leads eventually to steady state multiplicity, a fact that will be shown to be determining for an acceptable precision of 1D models.

The abnormal behavior is introduced by strong self-inhibition effects or, for exothermic reactions, by temperature rise inside the pellet. Thus, we employ in this study irreversible kinetic expressions of the type  $\pi_A(C_A, T) = k(T)C_A^n/(1 + K_{ad}C_A)^d$ , with Arrhenius expression  $k(T) = k_0 \exp(-E/RT)$ .



Table 2. Shape Parameters for 3D Pellets in Table 1 and Parameter Values of 1D Approximations for an Irreversible First-Order Exothermic Reaction ( $\delta = 4.0$ ,  $n = 1$ ,  $d = 0$  in eq 23a)

	parameter	pellet				
		4-holes	trilobe	10-holes	wagon wheel	modified 4-holes
3D pellet	$\Gamma$	0.196	0.795	-0.034	0.337	0.150
	$\gamma$	0.448	0.623	0.368	0.447	0.386
	$\beta$	0.290	0.566	0.179	0.305	0.194
1D-GC $\gamma$	$\sigma$	0.622	2.311	0.166	0.619	0.256
1D-GC $\Gamma$	$\sigma$	0.243	3.872	-0.033	0.508	0.176
1D-VD	$\alpha$	6.380	4.600	7.880	13.86	11.74
	$C_1$	-0.391	-1.540	0.069	-0.673	-0.300
	$C_2$	-6.230	-3.077	-6.836	-9.132	-7.549

The coefficient  $K_{ad}$  (that can be interpreted as an adsorption constant) was assumed independent of  $T$ . Also, the effect of the structure of reversible kinetics was studied by considering a reaction  $A \leftrightarrow B$  with  $\pi_A(C_A, T) = k(T)(C_A^2 - C_B^2/K_{eq})$ , where the equilibrium constant  $K_{eq}$  is taken as a parameter, rather than temperature dependent. From these rate expressions and taking into account eq 1a for  $C_B$  (considering  $C_{Bs} = 0$  and  $D_A/D_B = 1$ ) and eq 1b for  $T$ , the dimensionless rate  $r(Y) = \pi_A/\pi_{A,s}$  can be expressed

Irreversible type

$$r(Y) = \exp\left[\frac{\delta(1-Y)}{1+\beta_p(1-Y)}\right] Y^n \left(\frac{1+\kappa}{1+\kappa Y}\right)^d \quad (23a)$$

Reversible type

$$r(Y) = \exp\left[\frac{\delta(1-Y)(1-C_{Ac}^*)}{1+\beta_p(1-Y)(1-C_{Ac}^*)}\right] Y \left[\frac{Y+2C_{Ac}^*(1-Y)}{1-C_{Ac}^*}\right] \quad (23b)$$

where  $\delta = \alpha_A \beta_p$ ,  $\alpha_A$  is the Arrhenius number  $E/(RT_s)$ ,  $\beta_p$  is the Prater number  $(-\Delta H_A)(D_A/\lambda)(C_{A,s}/T_s)$ ,  $\kappa = K_{ad}C_{A,s}$  and  $C_{Ac}^* = C_{Ac}/C_{A,s}$ .

For the present calculations the denominator in the exponential arguments was taken as being the unity, because  $\beta_p$  is usually a small number ( $|\beta_p| < 0.1$  is a normal range). Therefore, the available parameters are  $\delta$ ,  $n$ ,  $d$  for irreversible kinetics and  $\delta$ ,  $C_{Ac}^*$  for reversible kinetics.

The *apparent reaction order* is defined as  $n_{ap} = d[\ln r(Y)]/d(\ln Y)$ . Abnormal behavior is found if  $n_{ap} < 0$  at least for some values of  $Y$  within the range  $0 < Y < 1$ . This is accompanied by the existence of values  $\eta > 1$  for some range of  $\Phi$  values. For eqs 23, this can happen when  $\delta$  is large enough (temperature rise effect) or, specifically for eq 23a and  $d > n$ , if  $\kappa$  is large enough (self-inhibition effect). In both cases, the minimum value of  $n_{ap}$  takes place for  $Y = 1$  (at the pellet surface); therefore, the sign of  $n_{ap}(1)$  determines the normal or abnormal behavior once  $r(Y)$  is given.

For a given 3D pellet, parameter  $\Gamma$  was evaluated from eq 10 from the geometric information reported in Table 1, while parameters  $\gamma$  and  $\beta$  were obtained from eqs 6 after solving eqs 7 with COMSOL Multiphysics software (numerical solution of differential equations by the finite elements method).

Values of  $\Gamma$ ,  $\gamma$ , and  $\beta$  for the pellet shapes in Table 1 and derived parameters of 1D models (eqs 16, 17, and 22) are displayed in Table 2 for an irreversible first-order exothermic reaction ( $\delta = 4$ ,  $n = 1$ ,  $d = 0$  in eq 23a). As discussed before, the effect of kinetics on shape parameters is mild (only on  $\Gamma$ ), a

feature that is transferred to parameters of the 1D models. Therefore, values in Table 2 are mainly inherent to the 3D pellet shape. The exponent  $\alpha$  of the 1D-VD model is mainly associated to the requirement of matching parameter  $\beta$  (eq 22c), which in turn describes the behavior at positions well inside the actual pellet catalyst, where  $G^2$  takes maximum values (eq 6b). Therefore, to capture this effect, values of  $\alpha$  becomes large (the effect of the term  $C_2 x^\alpha$  in eq 21 is maximum close to  $x = 1$ , i.e. close to the middle of the slab).

COMSOL Multiphysics was also used for solving the mass balance of the actual 3D pellets (eqs 2) and then the effectiveness factor evaluated from eq 4. Instead, a routine developed in our group that is based on a shooting procedure to solve an integral formulation of the 1D conservation equations (eqs 12 for the 1D-GC model and 19 for the 1D-VD model) was employed to evaluate the approximate effectiveness factors, eqs 13 and 20. Either for evaluating the actual or approximate values of  $\eta$ , the size of the mesh for numerical evaluation was adjusted to guarantee accuracy of about 0.1%.

To evaluate the precision of 1D models, the relative error  $\varepsilon$  in estimating the effectiveness factor ( $\eta$ ) is defined by

$$\varepsilon = 100 \frac{\eta^m - \eta}{\eta} \quad (24)$$

where  $\eta$  stands for the effectiveness factor of an actual 3D pellets and  $\eta^m$  for the value obtained from either 1D-VD or 1D-GC models.

According to the criteria employed to adjust model parameters in both cases, 1D-VD and 1D-GC, maximum errors (denoted by  $\varepsilon_{max}$ ) will take place for an intermediate value of Thiele modulus. For the most part, these maxima have been employed as a criterion to assess 1D models precision for each kinetic expression and 3D pellet shape:

$$\varepsilon_{max} = \max_{\Phi} \{|\varepsilon|\} \quad (25)$$

As commented on before, the one parameter 1D-GC model has been found able to approximate the behavior of a great variety of pellet shapes with relative dimensions taken from manufactures' information, within 3% of error for normal kinetics.<sup>7,8</sup> Isothermal zero-order kinetics can be considered as the boundary between normal and abnormal reaction behavior ( $n_{ap} = 0$ ). An isothermal zero-order reaction arises from eq 23a by taking  $\delta = 0$ ,  $n = d$ ,  $\kappa \rightarrow \infty$ , thus resulting in  $r(Y) = 1$  if  $Y > 0$ ,  $r(Y) = 0$  if  $Y = 0$ . Therefore, it is important to explore as a first step the performance of the 1D models in this case. Table 3 shows  $\varepsilon_{max}$  for the pellet cross-section shapes in Table 1, but with  $H \rightarrow \infty$ , as this is the more severe case for 1D-models. The 1D-GC model ( $\gamma$  or  $\Gamma$ ) leads, except for the particular case

**Table 3. Maximum Errors ( $\epsilon_{\max}$ ) in the Prediction of Effectiveness Factor ( $\eta$ ) Using 1D Approximations for Infinite Pellet Height ( $H \rightarrow \infty$ ) Running an Irreversible Zero-Order Reaction**

kinetic expression	model	pellet				
		4-holes	trilobe	10-holes	wagon wheel	modified 4-holes
irreversible zero-order reaction ( $\delta = 0, n = d, \kappa \rightarrow \infty$ )	1D-VD	1.6	1.3	1.3	0.7	1.1
	1D-GC $\gamma$	6.4	0.2	5.1	6.4	2.8
	1D-GC $\Gamma$	14.0	0.8	15.8	6.4	7.4

of the trilobe pellet, to values of  $\epsilon_{\max}$  considerably larger than 3% (the level found for normal kinetics). On the contrary, results from 1D-VD model can be considered completely satisfactory, as  $\epsilon_{\max}$  is maintained well below 2%.

For a given pellet shape and type of kinetic expression, as those in eqs 23, a critical parameter can be chosen (e.g.,  $\delta$  or  $\kappa$ ) to vary the apparent reaction order from positive (normal behavior) to negative values, until steady state multiplicity is reached. In this sequence, values  $\epsilon_{\max}$  of 1D approximations show, in general, an increasing trend and they rapidly rise as multiplicity is being approached. This behavior can be clearly appreciated in Figure 1 for the particular case of wagon wheel

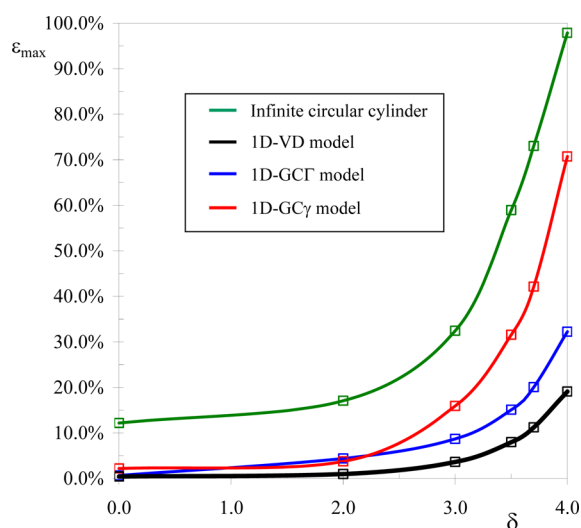


**Figure 1.**  $\epsilon_{\max}$  vs  $\delta$  for the wagon wheel pellet from Table 1 ( $h = 1$ ). Irreversible first-order exothermic kinetic expression ( $n = 1, d = 0, \delta \neq 0$  in eq 23a).

pellet (Table 1) with  $h \rightarrow 1$  and for an irreversible exothermic first-order reaction (i.e.,  $n = 1, d = 0, \delta \neq 0$  in eq 23a). Values of  $\epsilon_{\max}$  for an infinitely long circular cylinder are also presented. As commented on in the Introduction, this 1D geometry can be an option to evaluate effective reaction rates if no provision is taken for the real shape of the catalytic pellet. For models 1D-GC $\gamma$ , 1D-GC $\Gamma$ , and 1D-VD,  $\epsilon_{\max}$  sharply increases as  $\delta$  approaches the value corresponding to the onset of multiplicity ( $\delta_{\text{om}} \cong 4.2$ ). The same trend is observed for the long circular cylinder, but even for the isothermal case ( $\delta = 0$ ),  $\epsilon_{\max}$  is above 12% and reaches values close to 100% at  $\delta \cong \delta_{\text{om}}$ . Other shapes and kinetic expressions varying their critical parameters were also tested showing the same trend.

We have analyzed specifically four rate expressions: the reversible expression eq 23b with  $C_{\text{Ac}}^* = 0.6$  and three irreversible kinetics derived from eq 23a.

Irreversible first-order exothermic reaction ( $n = 1, d = 0$ )

$$r(Y) = Y \exp[\delta(1 - Y)]$$

Irreversible second-order exothermic reaction ( $n = 2, d = 0$ )

$$r(Y) = Y^2 \exp[\delta(1 - Y)]$$

Self-inhibited isothermal reaction ( $\delta = 0, n = 1, d = 2$ )

$$r(Y) = Y \left( \frac{1 + \kappa}{1 + \kappa Y} \right)^2$$

In the first three cases, the critical parameter is  $\delta$  and for the fourth example the role is played by  $\kappa$ . As the onset of multiplicity varies slightly with geometry, the slab geometry with uniform diffusivity was (rather arbitrarily) chosen to characterize each of the four kinetic expressions with a definite value of the critical parameter for the onset of multiplicity.

Values of  $\epsilon_{\max}$  from 1D models for the four examples of kinetic expressions and for pellet shapes and dimensions in Table 1 (specifically, for the finite heights defined by parameter  $h$  in Table 1) and for critical parameters amounting around 95% of the values for the onset of multiplicity are displayed in Table 4. It can be clearly appreciated that errors from the 1D-VD model remain smaller than around 10%. On the other hand, the 1D-GC model (irrespective of the criterion used to fix parameter  $\sigma$ ) shows values of  $\epsilon_{\max}$  even higher than 40%.

Similar calculations as those in Table 4 were performed for pellets with  $H \rightarrow \infty$  and for critical parameters about 90% (rather than 95%) of those leading to multiplicity (Table 5). Basically, the same comments as for Table 4 can be made for the results of  $\epsilon_{\max}$  in Table 5. Actually, the slightly larger departure (from 95 to 90%) from the onset of multiplicity has to be made for keeping nearly the same level of maximum errors than in Table 4, since long pellets, in general, tend to emphasize the effect of shape, as discussed before.

The results in Tables 4 and 5 demonstrate that 1D-VD model is capable to predict effective reaction rates with maximum errors bounded by around 10% for the whole range of Thiele modulus if critical parameters are kept below 90–95% of the values leading to the onset of steady state multiplicity. On the other hand, the 1D-GC model can introduce unacceptable large errors; however, it can still be appropriate for some shapes, as revealed by results of trilobe pellets and 1D-GC $\gamma$  model (Tables 4 and 5). Nonetheless, the possibility of employing the 1D-GC model will need a previous study performed on the specific 3D pellet shape.

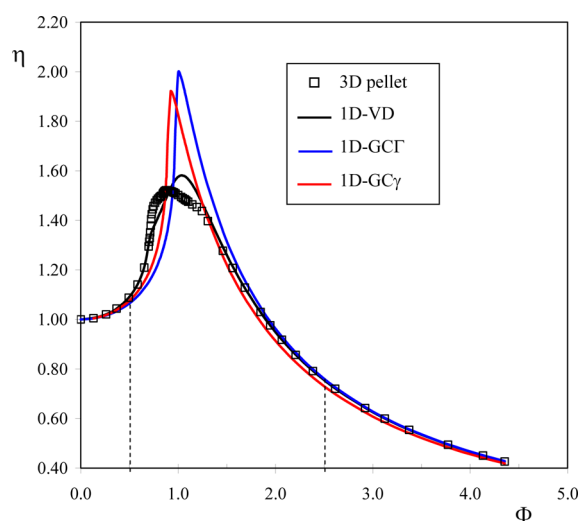
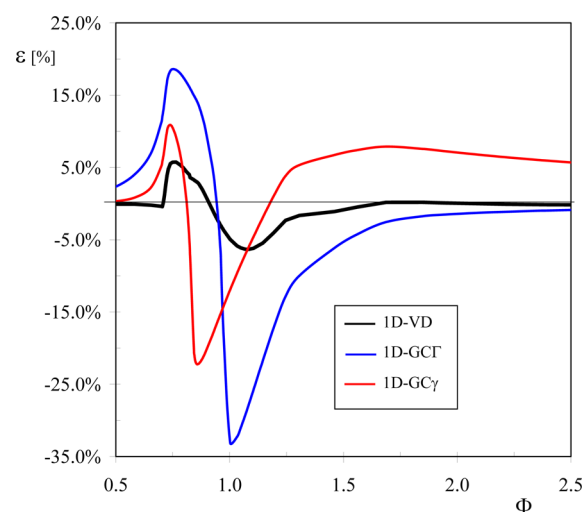
The magnitude  $\epsilon_{\max}$  is a stringent measure for assessing the behavior of 1D approximations, since it arises from detecting the Thiele modulus at which the maximum error is reached. These values of Thiele modulus invariably are close to one. In many problems, it is likely that relevant values of  $\Phi$  lie outside the region that gives rise to  $\epsilon_{\max}$ . Therefore, it is important to explore the behavior of the approximate models in the whole range of  $\Phi$ . Figure 2 presents values of  $\eta$  vs  $\Phi$  for the 4-holes pellet (Table 1) with infinite height ( $h = 1$ ) and self-inhibited isothermal reaction ( $\delta = 0, n = 1, d = 2, \kappa = 8$  in eq 23a). The 1D-VD model follows the results of the actual pellet very tightly at both sides of the region around the maximum of  $\eta$ , where  $\epsilon_{\max}$  takes place. On the other hand, the 1D-GC not only introduces differences in that region, but the errors are also

**Table 4. Maximum Errors ( $\epsilon_{\max}$ ) in the Prediction of Effectiveness Factor ( $\eta$ ) using 1D Approximations for Commercial Pellets (Finite Height) and Different Abnormal Kinetic Expressions**

kinetic expression	model	pellet				
		4-holes	trilobe	10-holes	wagon wheel	modified 4-holes
irreversible first-order exothermic reaction ( $\delta = 4, n = 1, d = 0$ )	1D-VD	11.0	3.3	11.1	5.2	8.2
	1D-GC $\gamma$	26.8	3.6	26.8	43.3	19.2
	1D-GC $\Gamma$	36.1	36.4	32.6	36.0	22.8
irreversible second order exothermic reaction ( $\delta = 5.5, n = 2, d = 0$ )	1D-VD	7.4	2.7	7.0	3.5	3.9
	1D-GC $\gamma$	21.7	2.4	18.6	30.6	12.9
	1D-GC $\Gamma$	31.7	25.2	27.7	24.1	15.2
reversible second-order exothermic reaction ( $\delta = 9.5, C_{Ae} = 0.6$ )	1D-VD	10.2	3.3	10.8	5.0	7.9
	1D-GC $\gamma$	26.5	3.5	26.2	42.4	18.7
	1D-GC $\Gamma$	36.0	35.8	32.2	35.1	22.2
irreversible self-inhibited reaction ( $\kappa = 9, n = 1, d = 2$ )	1D-VD	6.2	2.7	5.5	3.3	6.7
	1D-GC $\gamma$	18.7	2.8	21.6	24.8	15.6
	1D-GC $\Gamma$	25.7	10.5	22.7	23.1	14.2

**Table 5. Maximum Errors ( $\epsilon_{\max}$ ) in the Prediction of Effectiveness Factor ( $\eta$ ) Using 1D Approximations for Infinite Pellet Height ( $h \rightarrow 1$ ) and Different Abnormal Kinetic Expressions**

kinetic expression	model	pellet				
		4-holes	trilobe	10-holes	wagon wheel	modified 4-holes
irreversible first-order exothermic reaction ( $\delta = 3.7, n = 1, d = 0$ )	1D-VD	8.3	1.7	7.6	11.2	3.1
	1D-GC $\gamma$	25.0	4.0	22.4	42.1	14.1
	1D-GC $\Gamma$	34.8	2.8	31.9	20.0	21.0
irreversible second-order exothermic reaction ( $\delta = 5.0, n = 2, d = 0$ )	1D-VD	5.8	1.3	2.6	6.0	1.1
	1D-GC $\gamma$	17.6	1.3	13.1	24.4	8.1
	1D-GC $\Gamma$	25.7	1.5	23.2	11.0	12.4
reversible second-order exothermic reaction ( $\delta = 9, C_{Ae} = 0.6$ )	1D-VD	9.1	2.2	9.7	13.0	3.9
	1D-GC $\gamma$	26.7	5.3	25.3	48.0	15.8
	1D-GC $\Gamma$	37.7	3.7	34.2	22.7	23.9
irreversible self-inhibited reaction ( $\kappa = 8, n = 1, d = 2$ )	1D-VD	6.3	2.0	5.8	9.1	4.4
	1D-GC $\gamma$	22.2	3.8	24.4	31.4	15.3
	1D-GC $\Gamma$	33.1	1.6	27.2	24.3	14.4

**Figure 2.**  $\eta$  vs  $\Phi$  for the 4-holes pellet from Table 1 ( $h = 1$ ). Self-inhibited isothermal kinetics ( $\delta = 0, n = 1, d = 2, \kappa = 8$ ).**Figure 3.**  $\epsilon$  vs  $\Phi$  for the 4-holes pellet from Table 1 ( $h = 1$ ). Self-inhibited isothermal kinetics ( $\delta = 0, n = 1, d = 2, \kappa = 8$ ).

significantly propagated either at high values of  $\Phi$  (in the case of the 1D-GC $\gamma$ ) or at low values (1D-GC $\Gamma$ ); i.e., in correspondence to the criterion adopted to fix the shape factor  $\sigma$ .

The distribution of errors shown in Figure 3, for the same conditions as those in Figure 2, allows further visualization of

the behavior of the three approximate models. To quantify the spreading of errors, we evaluated the average error

$$\epsilon_{\text{av}} = \int_{\Phi_1}^{\Phi_2} |\epsilon| d\Phi / (\Phi_2 - \Phi_1)$$

in the range  $0.5 < \Phi < 2.5$  of Figure 2. Values of  $\varepsilon_{av}$  are 11.3, 13.0, and 2.85% for the 1D-GC $\gamma$ , 1D-GC $\Gamma$ , and 1D-VD models, respectively. Thus, it can be concluded that the 1D-VD model not only assures acceptable maximum errors ( $\varepsilon_{max}$ ), but it achieves a high level of precision within the whole range of  $\Phi$ .

The same kind of behavior as that analyzed on the basis of Figures 2 and 3 holds qualitatively for the other pellet shapes, heights, and kinetics studied.

One additional aspect that deserves attention concerns the criteria used to obtain parameter  $\sigma$  in the 1D-GC model. The results discussed above show that the 1D-GC model with its single parameter  $\sigma$  adjusted using the low- $\Phi$  (1D-GC $\gamma$ ) or high- $\Phi$  (1D-GC $\Gamma$ ) series expansion cannot produce accurate results for abnormal kinetics. However, it can be thought that the lack of precision may arise from the criteria employed rather than from the own structure of the model. To clarify this point, having available the exact results for each of the 3D pellet shapes,  $\sigma$  can be fixed using a direct optimization criterion. To this end, we have chosen the minimization of  $\varepsilon_{max}$ . A representative example of the results obtained in this way is provided by Figure 4, where values of  $\eta$  for the wagon wheel

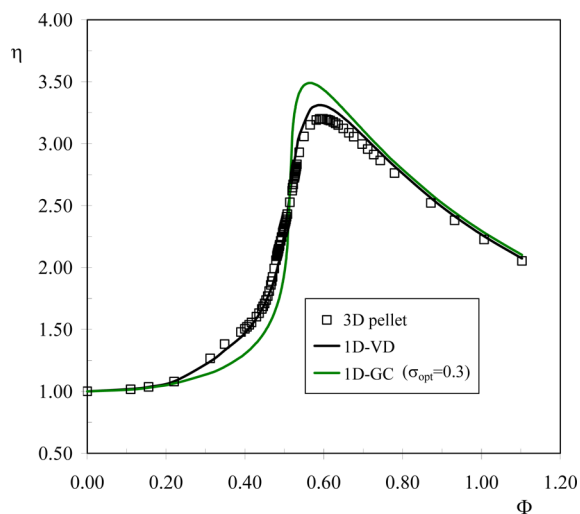


**Figure 4.** Comparison of values of  $\eta$  from the optimally adjusted 1D-GC model, values from 1D-VD model, and numerical values for the wagon wheel pellet with finite height (Table 1). Irreversible first-order exothermic kinetic expression ( $\delta = 4.0$ ,  $n = 1$ ,  $d = 0$ , eq 23a).

pellet (finite height in Table 1) and irreversible first-order exothermic kinetic expression ( $\delta = 4.0$ ,  $n = 1$ ,  $d = 0$ , eq 23a) are compared to values from the 1D-GC model with optimized  $\sigma$  and from the 1D-VD model. It is evident from Figure 4 that even using the best possible value of  $\sigma$ , the 1D-GC model cannot predict values of  $\eta$  with similar precision as the 1D-VD model can [ $\varepsilon_{max}^{1D-GC(\sigma_{opt}=0.3)} = 19.2\%$  vs  $\varepsilon_{max}^{1D-VD} = 5.2\%$ ].

## 5. CONCLUSIONS

Two different 1D models intended to approximate the behavior of 3D catalyst pellets have been evaluated in this contribution for abnormal kinetics expressions: a three-parameter model identified as the variable diffusion model (1D-VD) and a one-parameter model called the generalized cylinder model (1D-GC). Parameters of both models are evaluated by matching the behavior of the actual 3D pellets at low and high reaction rates (i.e., low and high Thiele modulus,  $\Phi$ ).

Several 3D pellets with shapes and dimensions taken from manufacturers were employed for the study. Both models were evaluated up to conditions close to the onset of steady state multiplicity, at which maximum levels of error are found. It has been shown that the applicability of the 1D-GC model, irrespective of the criterion chosen to fix its parameter, lead at the most stringent conditions to errors of up to near 50% in the estimation of the effectiveness factor. Taking into account results from previous contributions, it can be concluded that the 1D-GC model can be employed with acceptable precision for normal kinetics, but its general use for abnormal kinetics cannot be recommended.

On the contrary, the 1D-VD model appears to be much more robust for dealing with abnormal kinetics, as it can be employed with suitable precision (maximum levels of errors in the order of 10%) even at conditions close to steady state multiplicity. The approach to the onset of multiplicity has been evaluated on the basis of a critical kinetic parameter identified as being the main cause of the abnormal behavior. If this critical kinetic parameter takes less than 90% of its value defining the onset of multiplicity, the 1D-VD model can be employed within the quoted level of precision. Maximum errors from 1D models take place close to the appearance of the maximum of effectiveness factor as a function of  $\Phi$ . Outside a small zone of  $\Phi$  around the value leading to the maximum, the errors from the 1D-VD model rapidly diminish and becomes essentially nil for most of the ranges of low and fast reactions.

A number of aspects deserve further studies to appraise comprehensively the capability of 1D models, being one of the most important the analysis of simultaneous multiple reactions, as the saving in computing time when using a one-dimensional approximation will be most significant.

## AUTHOR INFORMATION

### Corresponding Author

\*E-mail: barreto@quimica.unlp.edu.ar.

### Notes

The authors declare no competing financial interest.

## ACKNOWLEDGMENTS

The authors wish to thank the following Argentine institutions for financial support: ANPCyT-MINCYT (PICT'11-1641), CONICET (PIP 0304), and UNLP (PID No. 11/I136). N.J.M., O.M.M., and G.F.B. are research members of CONICET. M.J.T. holds a grant from CONICET.

## REFERENCES

- (1) Aris, R. A Normalization for the Thiele modulus. *Ind. Eng. Chem. Fundam.* **1965**, *4*, 227–229.
- (2) Datta, R.; Leung, S. W. K. Shape generalized isothermal effectiveness factor for first-order kinetics. *Chem. Eng. Commun.* **1985**, *39* (1), 155–173.
- (3) Macías Hernández, M. J.; Morales, R. D.; Ramírez-Lopez, A. Simulation of the Effectiveness Factor for a Tri-Lobular Catalyst on the Hydrodesulfurization of Diesel. *Int. J. Chem. Reactor Eng.* **2009**, *7* (1), 1–21.
- (4) Lopes, J. P.; Cardoso, S. S. S.; Rodrigues, A. E. Effectiveness factor for thin catalytic coatings: Improved analytical approximation using perturbation techniques. *Chem. Eng. Sci.* **2012**, *71*, 46–55.
- (5) Mariani, N. J.; Keegan, S. D.; Martínez, O. M.; Barreto, G. F. A one-dimensional equivalent model to evaluate overall reaction rates in catalytic pellets. *Chem. Eng. Res. Des.* **2003**, *81* (Part A), 1033–1042.
- (6) Mariani, N. J.; Keegan, S. D.; Martínez, O. M.; Barreto, G. F. On the evaluation of effective reaction rates on commercial catalyst by



means of a one-dimensional model. *Cat. Today* **2008**, 133–135, 770–774.

(7) Mariani, N. J.; Mocciaro, C.; Keegan, S. D.; Martínez, O. M.; Barreto, G. F. Evaluating the effectiveness factor from a 1D approximation fitted at high Thiele modulus: Spanning commercial pellet shapes with linear kinetics. *Chem. Eng. Sci.* **2009**, 64 (11), 2762–2766.

(8) Mariani, N. J.; Mocciaro, C.; Keegan, S. D.; Martínez, O. M.; Barreto, G. F. Estimation of effectiveness factor for arbitrary particle shape and non-linear kinetics. *Ind. Eng. Chem. Res.* **2009**, 48 (3), 1172–1177.

(9) Mocciaro, C.; Mariani, N. J.; Martínez, O. M.; Barreto, G. F. A three parameter one-dimensional model to predict effectiveness factor for an arbitrary pellet shape with linear kinetics. *Ind. Eng. Chem. Res.* **2011**, 50, 2746–2754.

(10) Keegan, S. D.; Mariani, N. J.; Martínez, O. M.; Barreto, G. F. Behavior of smooth catalyst at high reaction rates. *Chem. Eng. J.* **2005**, 110, 41–56.

(11) Keegan, S. D.; Mariani, N. J.; Martínez, O. M.; Barreto, G. F. Behavior of catalytic pellets at high reaction rates. The effect of the edges. *Ind. Eng. Chem. Res.* **2006**, 45, 85–97.

(12) Stewart, W. E. Invariant solutions for steady diffusion and reaction in permeable catalysts. *Chem. Eng. Sci.* **1978**, 33, 547–553.

(13) Aris, R. *The mathematical theory of diffusion and reaction in permeable catalysts*; Oxford University Press: London, 1975.

(14) Mocciaro, C. *Fenómenos de transporte en reactores trickle-bed*. Doctoral thesis, Universidad Nacional de La Plata, La Plata, Argentina, 2010.